Molecular Crystals and Liquid Crystals

ISSN: 1542-1406 (Print) 1563-5287 (Online) Journal homepage: http://www.tandfonline.com/loi/gmcl20

Structural, Nonlinear Absorption, and Optical Limiting Properties of a New Organic Crystal 3-(3-fluorophenyl)-1-[4-(methylsulfanyl) phenyl] prop-2-en-1-one

S. Raghavendra, C. S. Dileep & S. M. Dharmaprakash

To cite this article: S. Raghavendra, C. S. Dileep & S. M. Dharmaprakash (2015) Structural, Nonlinear Absorption, and Optical Limiting Properties of a New Organic Crystal 3-(3-fluorophenyl)-1-[4-(methylsulfanyl) phenyl] prop-2-en-1-one, Molecular Crystals and Liquid Crystals, 609:1, 192-204, DOI: 10.1080/15421406.2014.954323

To link to this article: http://dx.doi.org/10.1080/15421406.2014.954323

Published online: 11 Apr 2015.

Mol. Cryst. Liq. Cryst., Vol. 609: pp. 192–204, 2015

ISSN: 1542-1406 print/1563-5287 online
DOI: 10.1080/15421406.2014.954323

Structural, Nonlinear Absorption, and Optical Limiting Properties of a New Organic Crystal 3-(3-fluorophenyl)-1-[4-(methylsulfanyl) phenyl] prop-2-en-1-one

S. RAGHAVENDRA,[1,*] C. S. DILEEP,[2]
AND S. M. DHARMAPRAKASH[1]

[1]Department of Studies in Physics, Mangalore University, Mangalore, India
[2]Department of Studies in Physics, University of Mysore, Mysore, India

This paper deals with the studies on synthesis, characterization, nonlinear absorption, and optical-limiting property of a new organic crystal 3-(3-fluorophenyl)-1-[4-(methylsulfanyl) phenyl] prop-2-en-1-one (FMP). Primary characterization of FMP samples were performed using FTIR, UV-Visible, and NMR Spectroscopy techniques. FMP crystallizes in monoclinic system with centrosymmetric space group $P2_1/n$. UV-Visible spectrum shows minimum absorption in the entire visible region. From the thermo gravimetric and differential scanning calorimetry, melting point of FMP was found to be 96°C and there was no phase transition below this temperature. Open aperture Z scan experiment of FMP showed a good nonlinear absorption and optical-limiting property.

Keywords Characterization; chalcones; crystal growth; nonlinear optical material

Introduction

Organic nonlinear optical (NLO) materials are widely used in three dimensional optical data storage, optical limiting (OL), amplitude and phase modulation, optical switching, harmonic generators etc. [1–3]. Overall, the organic materials chalcones are identified for its large nonlinear optical coefficient, crystal stability, excellent blue light transmittance and remarkable OL property with nanosecond laser [4,5]. Π conjugated structure (alternative single and double bond for delocalization of electron) with donor and acceptors on aromatic rings at the end of the molecule is very essential to achieve NLO property [6]. Chalcones belongs to flavonoids class, having π conjugated structure and two aromatic rings are interconnected by a chain of α, β unsaturated carbon atoms and carbonyl groups [7]. The nonlinear optical materials having OL property exhibits intensity dependent nonlinear absorption, popularly known as optical limiter that limits or blocks high intensity light and transparent to low intensity light [8]. OL property can be achieved by several nonlinear process like two photon absorption (TPA), reverse saturable absorption (RSA), excited state absorption (ESA) [9]. In this paper, we report synthesis, crystal structure, spectroscopic,

*Address correspondence to S. Raghavendra, Department of Studies in Physics, Mangalore University, Mangalore, India. E-mail: raghuphotonics@gmail.com

Color versions of one or more of the figures in the article can be found online at www.tandfonline.com/gmcl.

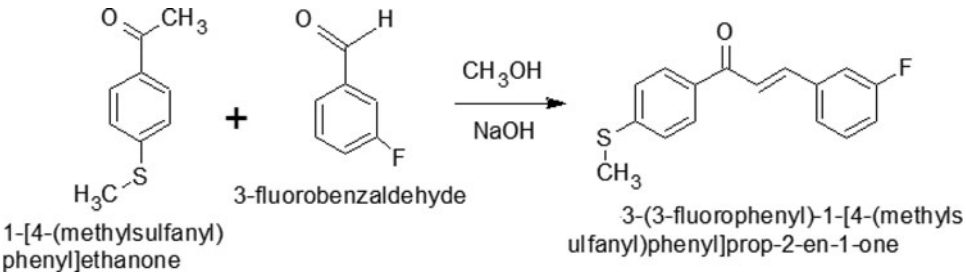

Figure 1. Synthesis route of FMP.

thermal study of a new nonlinear organic crystal 3-(3-fluorophenyl)-1-[4-(methylsulfanyl) phenyl] prop-2-en-1-one (FMP). We also report optical nonlinear absorption and OL property of FMP crystal in DMF solution using frequency doubled Nd-YAG laser of wavelength 532 nm.

Material Synthesis and Crystal Growth

FMP was synthesized using standard procedure described in the literature [10]. Commercially available 3-flourobenzaldehyde and 4′-methylthioacetophenone (0.01 M each) were used to prepare FMP. These aldehyde and ketone were stirred in conical flask containing methanol and while stirring 20% of NaOH solution was added. Constant temperature was maintained during the entire reaction. After completion of reaction, mixture was poured in to clean beaker containing ice cold water. Synthesis route of FMP is shown in Fig. 1. Single Crystals of FMP grown from mixture of acetone and methanol solution are shown in Fig. 2. FMP crystals are nonhygroscopic and stable at room temperature.

Figure 2. Photograph of FMP crystals.

Nuclear Magnetic Resonance Study

Proton NMR (^{1}H NMR) and carbon NMR (^{13}C NMR) spectra of FMP crystals were recorded using Bruker AV 400-NMR spectrometer in $CDCl_3$ solution. TMS was used as an internal standard. ^{1}H NMR and ^{13}C NMR spectra are presented in Figs. 3 and 4. Different chemical shifts are presented in terms of ppm (parts per million). Proton resonance multiplicities in ^{1}H NMR are designated as singlet (s), doublet (d) and multiplet (m).The characteristic peaks observed for ^{1}H NMR and ^{13}C NMR of FMP crystals were described as follows;

^{1}H NMR (400 MHz, $CDCl_3$): δ, 2.53(s, 3H, -SCH_3), 7.08–7.12 (m, 1H, 3-Fluorophenyl-6-H), 7.26-7.39 (m, 5H, 3-Fluorophenyl-(2,4,5)-H & 4-Methylthiophenyl-(3,5)-H) 7.51(d, 1H, propenone-3-H, J = 15.6Hz), 7.76 (d, 1H, propenone-2-H, J = 15.6Hz), 7.96 (d, 2H, 4-Methylthiophenyl-(2,6)-H), J = 8Hz);

^{13}C NMR(400MHz) : δ, 14.73 (SCH_3 carbon), 114.38, 117.25 (Aromatic carbon atoms), 122.82 (Propenone-3-C), 124.51, 125.03, 128.93, 130.42, 130.50, 134.07, 137.14 (Aromatic carbon atoms), 142.9 (d, Propenone-2-C),146.0 (3-F-phenyl-3-C),188.76 (Carbonyl carbon).

FTIR Analysis

FTIR spectrum of FMP was recorded by Prestige-21 Shimadzu FTIR spectrophotometer and spectrum is shown in Fig. 5. Carbonyl (C=O) stretching vibrations generally observed in the range 1850 cm^{-1} to 1600 cm^{-1} [11]. As expected, the C=O band was observed at 1657 cm^{-1}, which confirmed the formation of the propenone (chalcone) between ketone and aldehyde. Aromatic C=C stretching vibration and C−H stretching vibration were observed at the band 1603 cm^{-1} and 3063 cm^{-1}, respectively. The band 1433 cm^{-1} corresponds to C−H deformation. The week absorption band due to aromatic C−S stretching (Ar−S−C) was observed at 662 cm^{-1} and the band 1243 cm^{-1} was assigned to C−F stretching.

Single Crystal XRD

The single crystal X-ray diffraction analysis was carried out using Bruker AXS Smart Apex II single crystal diffractometer. Compound crystallizes in monoclinic centrosymmetric space group $P2_1/n$, with unit cell parameters, $a = 11.1443$ Å, $b = 5.6292$ Å, $c = 21.6379$ Å and $\beta = 94.263^0$. FMP is almost planar with dihedral angle 3.19° between phenyl and benzoil rings, which is nearly 15 times smaller than 1-(4-bromophenyl)-3-[4(methylsulfanyl)phenyl]prop-2-en-1-one (4Br4MSP) [12] .The methylthio group attached at C1 is also nearly coplanar with C4-C5 ring with C16-S1-C1-C2 torsion angle 3.21°. Ortep diagram with 50% probability is shown in Fig. 6. Molecules are stabilized by C−H . . . O and C−F . . . H interactions. Packing diagram of FMP viewed down the *b* axis is shown in Fig. 7. Table 1 shows single crystal data and refinement of FMP crystal. Bond lengths, bond angles, and torsion angles are presented in Tables 2–4, respectively.

UV-Visible Study

The UV Visible spectrum of FMP crystals was recorded in DMF solution, using Shimadzu 1800 UV-Visible Spectrophotometer. In order to get linear absorption of pure compound, absorption contribution from both solvent and cuvette were subtracted. The resulted spectrum is shown in Fig. 8. In general, chalcones absorb light in UV region and transmits light in remaining region [4]. As expected FMP showed good

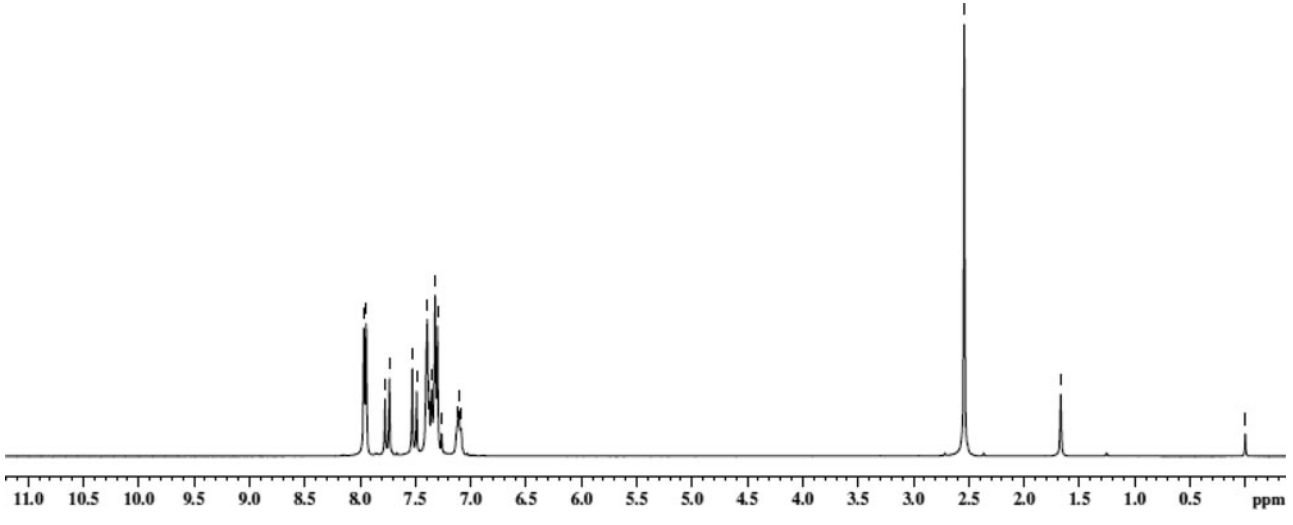

Figure 3. 1H NMR spectrum of FMP.

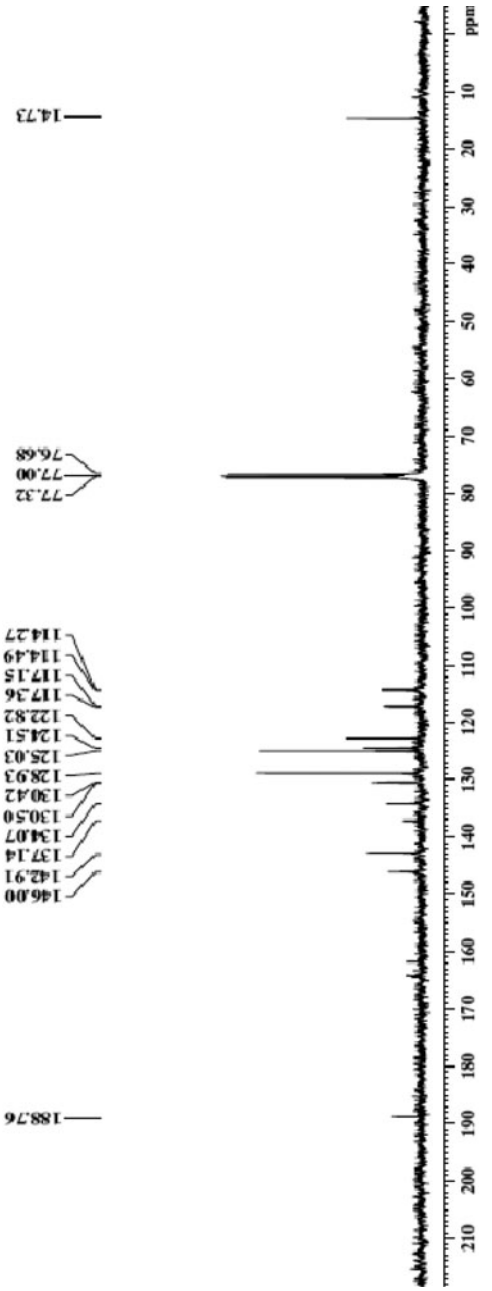

Figure 4. ^{13}C NMR spectrum of FMP.

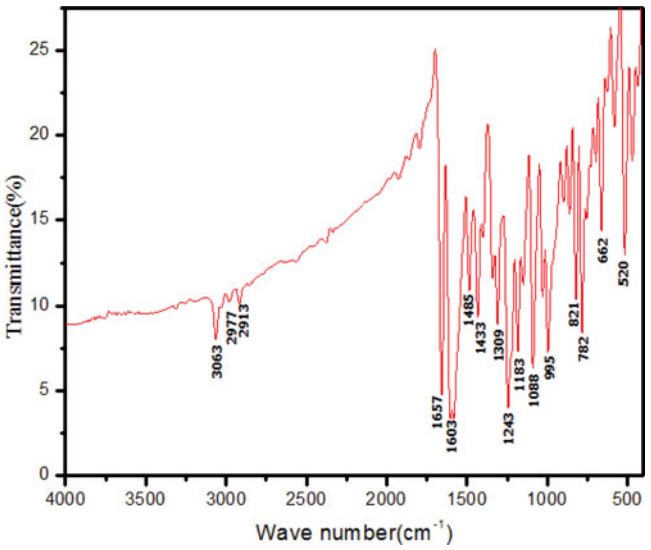

Figure 5. FTIR Spectrum of FMP.

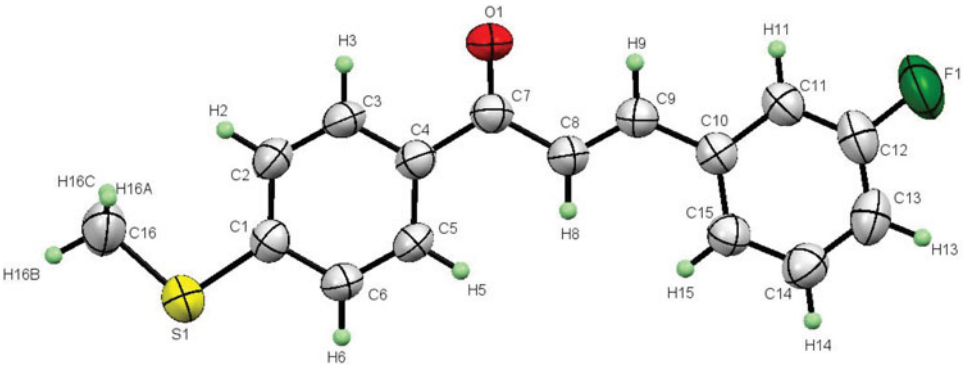

Figure 6. Ortep diagram of FMP.

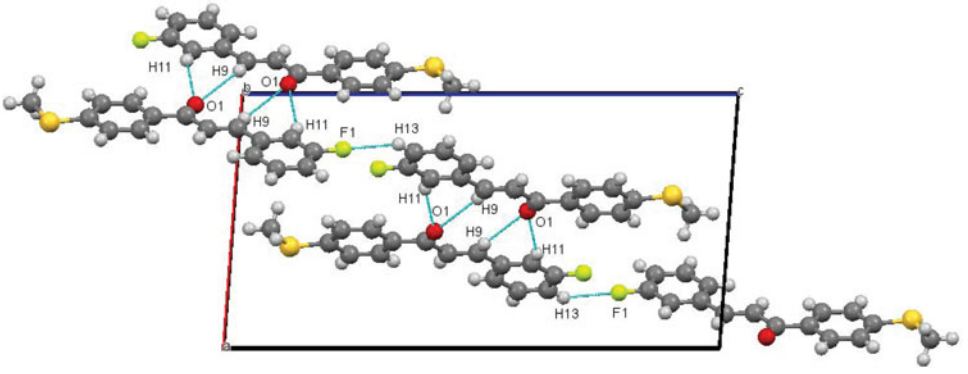

Figure 7. Packing diagram of FMP viewed down the *b* axis.

Table 1. Single crystal data and refinement, (CCDC No: 1005313)

Chemical formula	C16 H13 F O S
Formula weight	272.33
Temperature	296(2) K
Wavelength	0.71073 Å
Volume	1353.67Å^3
Z	4
Density (calculated)	1.336 mg/cm^3
Absorption coefficient	0.239 mm^{-1}
Index ranges	$-14<=h<=14$, $-6<=k<=7$, $-27<=l<=25$
Refinement method	Full-matrix least-squares on F2
Structure Solution technique	Direct method
Refinement program	SHELXL-97 (Sheldrick, 2008)
Goodness-of-fit on F2	1.053
$F(000)$	568
Independent reflections	2805 [R(int) = 0.0217]
Theta range for data collection	1.89 to 26.60°
Absorption correction	multi-scan

transparency in entire visible region. Maximum absorption in linear absorption spectrum can be assigned to n-π^*, π-π^* transitions, and may be attributed to aromatic ring and C=O (carbonyl) group excitation [13]. Cut off wavelength is found to be 402 nm. Beyond cut off wavelength, FMP is almost transparent and because of this transparency in visible region FMP can be made useful in nonlinear optical device applications.

TGA-DSC Analysis

The variation of weight loss and heat flow of FMP crystals was studied using simultaneous thermo gravimetric analyzer (TGA) and differential scanning calorimeter (DSC) in the temperature range 30°C to 600°C at the heating rate of 20°C/min in nitrogen atmosphere using SDTQ Simultaneous TGA/DSC analyzer. Figure 9 represents the TGA-DSC thermograms. TGA curve shows that FMP is stable up to 200°C. Decomposition (weight loss) of material starts nearly at 200°C and become maximum at 380°C. The peak at 96°C corresponds to melting point of the compound and it is slightly higher than the reported value for nonlinear second harmonic crystal (2E)-3-[4-(methylsulfanyl) phenyl]-1-(3-bromophenyl) prop-2-en-1-one (3Br4MSP).Thermal analysis suggests that FMP may be utilized for nonlinear device applications in the temperature range below its melting point.

Nonlinear Absorption and OL Property

FMP crystallizes in centrosymmetric space group P21/n, and second-order optical nonlinearity is absent in this material [14]. Hence open aperture Z scan experiment was carried out to study the third-order nonlinear optical phenomena namely, nonlinear absorption and OL property. For open aperture z scan experiment, solution of FMP in DMF was taken in 1 mm quartz cuvette (Optica, Japan) and irradiated by 5 ns Nd: YAG laser pulses at

Table 2. Bond lengths in Å

Atoms	Atoms	Bond Length
S1	C1	1.755(2)
S1	C16	1.781(4)
C4	C7	1.491(3)
C4	C5	1.397(3)
C4	C3	1.384(3)
C7	C8	1.466(3)
C7	O1	1.217(3)
C8	H8	0.929
C8	C9	1.323(3)
C6	H6	0.93
C6	C5	1.367(3)
C6	C1	1.393(3)
C9	H9	0.93
C9	C10	1.467(3)
C5	H5	0.929
C10	C11	1.389(3)
C10	C15	1.390(3)
C11	H11	0.93
C11	C12	1.369(4)
C2	H2	0.93
C2	C3	1.367(4)
C2	C1	1.387(3)
C3	H3	0.93
C15	H15	0.931
C15	C14	1.384(4)
C13	H13	0.931
C13	C14	1.373(4)
C13	C12	1.364(5)
F1	C12	1.360(3)
C14	H14	0.93
C16	H16A	0.96
C16	H16B	0.96
C16	H16C	0.96

the 532 nm wavelength at input energy 200 μJ. Concentration of solution used was 0.02 mole/cm^3.

For Gaussian beam, input fluence varies with position 'z' and it is given by

$$E(z) = {}^{4\sqrt{\ln 2 E_{in}}}\Big/_{\pi^{3/2}\omega(z)^2} \quad (1)$$

Where w (z) is the beam radius and E_{in} input beam energy. The intensity is obtained by dividing fluence with the pulse width of the laser. Figure 10 shows variation of normalized transmittance as a function of the input intensity. At lower irradiance, the FMP responds

Table 3. Bond angles in degree

Atom	Atom	Atom	Angle	Atom	Atom	Atom	Angle
C1	S1	C16	104.5(1)	H2	C2	C1	119.8
C7	C4	C5	123.3(2)	C3	C2	C1	120.4(2)
C7	C4	C3	119.1(2)	C4	C3	C2	121.9(2)
C5	C4	C3	117.6(2)	C4	C3	H3	119.1
C4	C7	C8	119.4(2)	C2	C3	H3	119
C4	C7	O1	119.8(2)	S1	C1	C6	116.6(2)
C8	C7	O1	120.8(2)	S1	C1	C2	125.1(2)
C7	C8	H8	119	C6	C1	C2	118.3(2)
C7	C8	C9	122.0(2)	C10	C15	H15	119.7
H8	C8	C9	118.9	C10	C15	C14	120.5(2)
H6	C6	C5	119.5	H15	C15	C14	119.8
H6	C6	C1	119.5	H13	C13	C14	121.1
C5	C6	C1	121.0(2)	H13	C13	C12	121.1
C8	C9	H9	116.7	C14	C13	C12	117.8(3)
C8	C9	C10	126.7(2)	C15	C14	C13	120.9(3)
H9	C9	C10	116.6	C15	C14	H14	119.6
C4	C5	C6	120.8(2)	C13	C14	H14	119.5
C4	C5	H5	119.6	C11	C12	C13	123.2(3)
C6	C5	H5	119.6	C11	C12	F1	117.6(3)
C9	C10	C11	118.8(2)	C13	C12	F1	119.3(3)
C9	C10	C15	122.8(2)	S1	C16	H16A	109.5
C11	C10	C15	118.4(2)	S1	C16	H16B	109.5
C10	C11	H11	120.4	S1	C16	H16C	109.5
C10	C11	C12	119.2(2)	H16A	C16	H16B	109.5
H11	C11	C12	120.4	H16A	C16	H16C	109.4
H2	C2	C3	119.8	H16B	C16	H16C	109.5

linearly to the incident intensity, and hence obeying Beer's law. But at higher irradiance, the curve departs from this law and the sample becomes less transparent [15]. This observation clearly indicates the OL effects of FMP. In Fig. 10, inset shows the open aperture z-scan curve obtained for FMP in DMF solution. Maximum nonlinear absorption at focus indicates the positive nonlinear absorption. Open aperture z-scan experimental data is fitted with the equation given in the literature [16]

$$\boldsymbol{T}(\boldsymbol{Z}, S = 1) = \frac{1}{\sqrt{\pi}\boldsymbol{q}_0(z, 0)} \int_{-\infty}^{\infty} \ln[1 + q_0(z, 0)e^{-\tau^2}]d\tau \tag{2}$$

When $|\mathbf{q_0}| < 1$, the transmittance equation can be expressed in summation form

$$T(z, S = 1) = \sum_{m=0}^{\infty} \frac{[(-q_0(z, 0))]^m}{(m + 1)^{\frac{3}{2}}} \tag{3}$$

Where the term $q_0(z, 0)$ is given by

Table 4. Torsion angles in degree

Atom	Atom	Atom	Atom	Torsion	Atom	Atom	Atom	Atom	Torsion
C16	S1	C1	C6	−178.3(2)	C8	C9	C10	C15	1.1(4)
C16	S1	C1	C2	3.2(3)	H9	C9	C10	C11	1.7
C1	S1	C16	H16A	−62.9	H9	C9	C10	C15	−178.9
C1	S1	C16	H16B	177.1	C9	C10	C11	H11	−2.2
C1	S1	C16	H16C	57.1	C9	C10	C11	C12	177.7(2)
C5	C4	C7	C8	1.4(3)	C15	C10	C11	H11	178.4
C5	C4	C7	O1	−176.2(2)	C15	C10	C11	C12	−1.6(4)
C3	C4	C7	C8	−179.2(2)	C9	C10	C15	H15	3.1
C3	C4	C7	O1	3.3(3)	C9	C10	C15	C14	−176.8(2)
C7	C4	C5	C6	177.0(2)	C11	C10	C15	H15	−177.6
C7	C4	C5	H5	−3	C11	C10	C15	C14	2.5(4)
C3	C4	C5	C6	−2.5(3)	C10	C11	C12	C13	0.1(4)
C3	C4	C5	H5	177.5	C10	C11	C12	F1	179.5(2)
C7	C4	C3	C2	−177.7(2)	H11	C11	C12	C13	−179.9
C7	C4	C3	H3	2.3	H11	C11	C12	F1	−0.6
C5	C4	C3	C2	1.8(4)	H2	C2	C3	C4	−179.6
C5	C4	C3	H3	−178.2	H2	C2	C3	H3	0.3
C4	C7	C8	H8	−2	C1	C2	C3	C4	0.3(4)
C4	C7	C8	C9	178.0(2)	C1	C2	C3	H3	−179.7
O1	C7	C8	H8	175.5	H2	C2	C1	S1	−3.4
O1	C7	C8	C9	−4.5(4)	H2	C2	C1	C6	178.2
C7	C8	C9	H9	−1	C3	C2	C1	S1	176.7(2)
C7	C8	C9	C10	179.0(2)	C3	C2	C1	C6	−1.8(4)
H8	C8	C9	H9	179	C10	C15	C14	C13	−1.9(4)
H8	C8	C9	C10	−1.1	C10	C15	C14	H14	178.2
H6	C6	C5	C4	−178.9	H15	C15	C14	C13	178.2
H6	C6	C5	H5	1.2	H15	C15	C14	H14	−1.7
C1	C6	C5	C4	1.1(3)	H13	C13	C14	C15	−179.7
C1	C6	C5	H5	−178.9	H13	C13	C14	H14	0.2
H6	C6	C1	S1	2.4	C12	C13	C14	C15	0.3(4)
H6	C6	C1	C2	−179	C12	C13	C14	H14	−179.8
C5	C6	C1	S1	−177.5(2)	H13	C13	C12	C11	−179.4
C5	C6	C1	C2	1.1(3)	H13	C13	C12	F1	1.2
C8	C9	C10	C11	−178.2(2)	C14	C13	C12	C11	0.6(5)

Where

$$q_o(z, 0) = \beta_{eff} L_{eff} I_o / \left(1 + z^2/z_o^2\right) \quad (4)$$

In equation (4) I_0 is being on axis peak irradiance at focus. z_0 is the Rayleigh length of sample and is given by $z_0 = \pi\omega_0^2/\lambda$, β_{eff} is effective nonlinear absorption coefficient; L_{eff} is effective thickness of the FMP solution. Effectiveness of the of OL can be determined by the figure of merit and materials having RSA property, figure of merit is given by the ratio of excited state absorption cross section (σ_{ex}) to the ground state absorption cross section

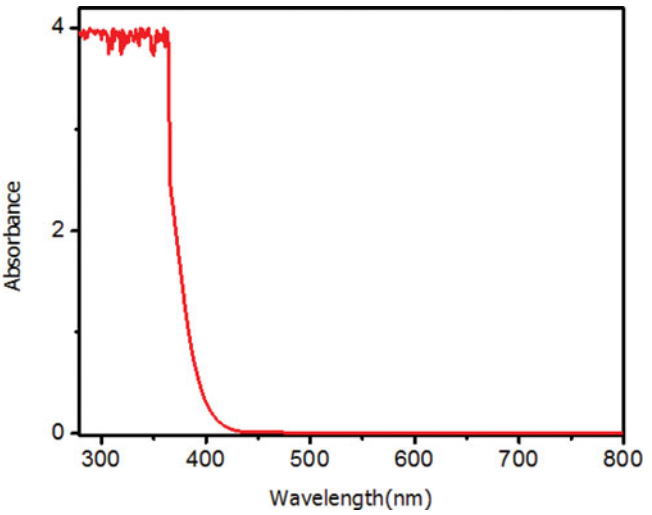

Figure 8. UV-Visible spectrum of FMP.

(σ_g) [17]. σ_{ex} can be calculated by fitting normalized open aperture data with the equation present in the literature [18]

$$T(z) = \frac{\ln\left(1 + {q_0}/{1 + x^2}\right)}{{q_0}/{1 + x^2}} \tag{5}$$

With $q_0 = \sigma_{ex} \times F_0 \times L_{eff} \times \alpha / 2\hbar\omega$

Where ω is angular frequency, α is linear absorption coefficient, $x = z^2/z_o^2$, F_0 is on axis fluence at the focus. σ_g can be calculated by the equation $\sigma_g = \alpha/N_A C$. Where N_A is Avogadro number and C is concentration in mol/cm^3. Calculated values β_{eff}, σ_{ex}, σ_g

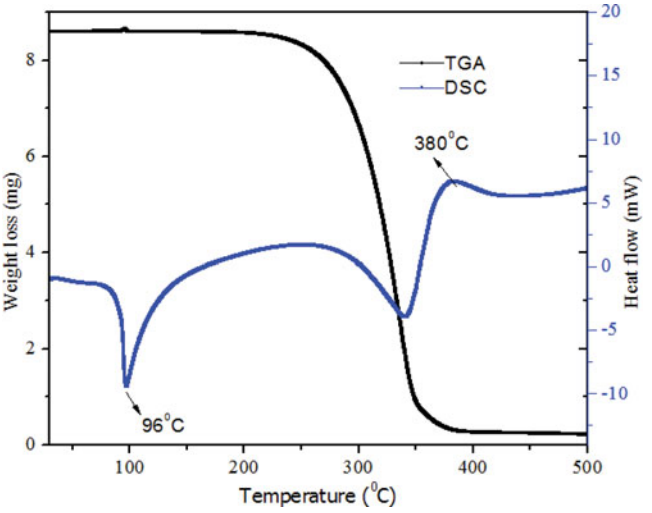

Figure 9. TGA-DSC thermogram of FMP.

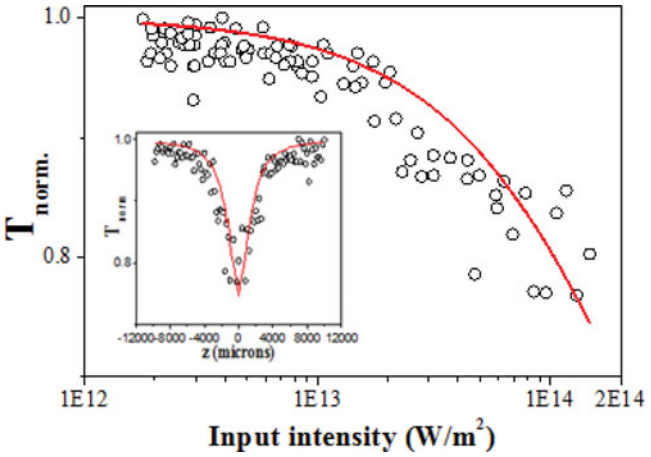

Figure 10. OL curve of FMP. Inset shows the open aperture z-scan curve. Circles and curves represent data points and numerical fit, respectively.

and figure of merit are given by 0.8 cm/GW, 8.7×10^{-17} cm^2, 2.63×10^{-22} cm^2 and 3.04×10^5 cm^2, respectively. The calculated σ_{ex} is greater than the value σ_g indicates that FMP is having RSA [19] and this may be the reason for exhibiting OL property [20]. The effective nonlinear absorption coefficient (β_{eff}) is comparable with reported organic compounds [3-(4,5-dimethoxy-2-nitrophenyl)-1-phenylprop- 2-en-1-ylidene]-N-(4-methyl phenoxy) acethydrazone and 4$^-$-methoxychalcone [21,22]. FMP molecule contains a strong electron donor 4-methylthio (SCH_3) phenyl ring in position—1 of propenone and an electron acceptor 3-fluorophenyl ring in position—3 of propenone. Being strong electron donor, SCH_3 group pushes electron towards electron accepting C=O group as well as electron acceptor 3-fluorophenyl ring. Charge transformation takes place from donor end to acceptor end of the molecule. FMP molecule belongs to D-A-A structure. Similar molecule 1-(4-methoxyphenyl)-3-(3-nitro-phenyl) prop-2-en-1-one, which showed strong RSA has been reported by Ravindra et.al. in order to study donor/acceptor strength on nonlinear optical property [22].

Conclusion

A new organic chalcone derivative: 3-(3-fluorophenyl)-1-[4-(methylsulfanyl) phenyl] prop-2-en-1-one (FMP) has been synthesized and crystallized by slow evaporation technique. Structure confirmation was done by NMR spectroscopy and functional groups present in FMP were confirmed by FTIR technique. Single-crystal XRD study reveals that FMP crystals belong to monoclinic system with centrosymmetric space group P21/n. The unit cell parameters of FMP crystal are: $a = 11.1443$ Å, $b = 5.6292$ Å, $c = 21.6379$ Å, and $\beta = 94.263^\circ$. Linear absorption spectral data collected show that FMP molecules are transparent in visible region beyond cut off wavelength. Melting point of the compound was found to be 96°C and absence of phase transition was observed before this temperature. Open aperture Z-Scan experiment revealed that the FMP molecule possess positive nonlinear absorption and optical-limiting property required for power limiting. Calculated values of excited state absorption cross section are much greater than the ground state absorption cross section

indicate that optical-limiting property of FMP molecule is due to RSA. Our work suggests that FMP can be exploited for optical sensor applications.

Acknowledgment

The authors thank the Co-ordinator, DST-FIST, Department of Physics for providing the experimental facility.

References

[1] Polyzos, I. et al. (2003). *Chem. Phys. Lett.*, *369*, 264.
[2] Uma, B., Das, S. J., Krishnan, S., & Boaz, B. M. (2011). *Phys. B Phys. Condens. Matter.*, *406*, 2834.
[3] Marder, S. R. et al. (1997). *Sci.*, *276*, 1233.
[4] Crasta, V. et al. (2005). *J. Cryst. Growth.*, *275*, e329.
[5] Janardhana, K., Ravindrachary, V., Rajesh Kumar, P. C., Yogisha, & Ismayil. (2013). *J. Cryst. Growth.*, *368*, 11.
[6] D'silva, E. D. et al. (2011). *J. Phys. Chem. Solids.*, *72*, 824.
[7] Waghmare, V. G., Kariya, K. P., & Paliwal, L. J. (2011). *J. Mater. Sci. Eng. B.*, *1*, 485.
[8] Pawlicki, M., Collins, H. A., Denning, R. G., & Anderson, H. A. (2009). *Angew. Chem. Int.*, *48*, 3244.
[9] Manjunatha, K. B., Dileep, R., Umesh. G., & Bhat, B. R. (2013). *Opt. Mater.*, *35*, 1366.
[10] Dhar, D. N. (1981). *Chemistry of Chalcones and Related Compounds*, Wiley: New York.
[11] Sudha, S., Sundaraganesan, N., Vanchinathan, K., Muthu, K., & Meenakshisundaram, S. (2012). *J. Mol. Struct.*, *1030*, 191.
[12] D'silva, E. D., Krishna Podagatlapalli, G., Venugopal Rao, S., & Dharmaprakash, S. M., (2012). *Mater. Res. Bull.*, *47*, 3552.
[13] Rajesh Kumar, P. C. et al. (2011). *J. Mol. Struct.*, *1005*, 1.
[14] Manjunath, H. R. et al. (2011). *J. Cryst. Growth.*, *327*, 161.
[15] Zhang, G., Cao, D., Liu, Z., & Li, G. (2008). *Acta Chim. Slov.*, *55*, 315.
[16] Sheik-Bahae, M., Said, A. A., Wei, T. H., Hagan, D. J., & Van Stryland, E. W. (1990). *IEEE J. Quantum Electron.*, *26*, 760.
[17] Haripadmam, P. C., Kavitha, M. K., John, H., Krishnan, B., & Gopinath, P. (2012). *Appl. Phys. Lett.*, *101*, 071103.
[18] Wood, G. L., Miller, M. J., & Mott, A. G. (1995). *Opt. Lett., 20*, 973.
[19] Tutt, L. W., & Boggess, T. F. (1993). *Prog. Quant. Electr.*, *17*, 299.
[20] Hea, T., Wang, C., Zhang, C., & Lu, G. (2011). *Phys. B Phys. Condens. Matter.*, *406*, 488.
[21] Vijayakumar, S., Babu, M., Kalluraya, B., & Chandrasekharan, K. (2012). *Opt. - Int. J. Light Electron Opt.*, *123*, 21.
[22] Ravindra, H. J., Kiran, A. J., Chandrasekharan, K., Shashikala, H. D., & Dharmaprakash, S. M. (2007). *Appl. Phys. B*, *88*, 105.